

Quasielastic Charged Current Neutrino-nucleus Scattering

J.E. Amaro

*Departamento de Física Atómica, Molecular y Nuclear,
Universidad de Granada, 18071 Granada, SPAIN*

M.B. Barbaro

*Dipartimento di Fisica Teorica, Università di Torino and INFN,
Sezione di Torino, Via P. Giuria 1, 10125 Torino, ITALY*

J.A. Caballero

Departamento de Física Atómica, Molecular y Nuclear, Universidad de Sevilla, 41080 Sevilla, SPAIN

T.W. Donnelly

*Center for Theoretical Physics, Laboratory for Nuclear Science and Department of Physics,
Massachusetts Institute of Technology, Cambridge, MA 02139, USA*

(Dated: September 5, 2019)

We provide integrated cross sections for quasielastic charged-current neutrino-nucleus scattering. Results evaluated using the phenomenological scaling function extracted from the analysis of experimental (e, e') data are compared with those obtained within the framework of the relativistic impulse approximation. We show that very reasonable agreement is reached when a description of final-state interactions based on the relativistic mean field is included. This is consistent with previous studies of differential cross sections which are in accord with the universality property of the superscaling function.

PACS numbers: 25.30.Pt; 13.15.+g; 24.10.Jv

The development of present and future experimental studies of neutrino oscillations at intermediate to high energies benefits from high-quality predictions for neutrino-nucleus cross sections. The kinematics involved in these processes typically lie in a domain where a fully relativistic formalism is required; not only should the reaction mechanism incorporate relativity, but also the nuclear dynamics must be described in a relativistic framework. Moreover, any reliable model of neutrino-nucleus scattering first needs to be tested against electron scattering for similar kinematics. Fully relativistic results for the latter have been presented in the past [1, 2, 3] using the impulse approximation, namely, where only one nucleon in the nucleus interacts with the virtual photon exchanged in the process. Such analyses have been shown to provide accurate descriptions of quasielastic (QE) *exclusive* ($e, e'p$) processes when a proper description of the final-state interactions (FSI) between the ejected nucleon and the residual nucleus is incorporated. This is accomplished by using complex relativistic optical potentials which have been fitted to elastic nucleon-nucleus scattering data [4]. For *inclusive* processes of the type (e, e') and (ν, μ), the contribution of all channels must be retained; hence the use of complex potentials should be avoided because of the loss of flux implied by the imaginary term. Different approaches have been considered in the literature, e.g., the use of purely real potentials within the impulse approximation [5, 6, 7] and analyses based on the Green function method [8, 9]. Although both treatments lead to similar results, a comparison with experimental QE cross sections is not yet conclusive because of the

effects introduced by ingredients beyond the impulse approximation such as long- and short-range correlations, meson-exchange currents (MEC) and, at high energies, the excitation of the Δ resonance.

These difficulties can be partially overcome by making use of the scaling behavior of the electron-nucleus cross sections through a SuperScaling Analysis (SuSA) in the region of both the QE and Δ peaks. Previous investigations of inclusive (e, e') world data have clearly demonstrated the validity of scaling and superscaling properties in these kinematical domains [10, 11, 12]. To summarize: by dividing the experimental (e, e') differential cross sections by an appropriate single-nucleon factor one gets the superscaling function, which embodies the basic information about the nuclear dynamics. At sufficiently high energies this function depends upon the transferred momentum (q) and energy (ω) only through a particular combination, the scaling variable $\psi(q, \omega)$ [11, 12] (first-kind scaling) and is independent of the particular nucleus selected (second-kind scaling).

Importantly, the superscaling function extracted from data presents an asymmetric shape with a pronounced tail extending into the region of high transferred energies, corresponding to positive values of the scaling variable ψ . While this asymmetry is largely absent in most non-relativistic models based on the impulse approximation, the systematic study presented in [6, 7] has shown that the correct amount of asymmetry is provided in the relativistic impulse approximation (RIA) when FSI are described with a relativistic mean field (RMF) potential. Recently, a similar asymmetric scaling function has also

been obtained within a semi-relativistic (SR) approach including FSI through a Dirac-equation-based model [13].

The superscaling function $f(\psi)$ has been investigated in detail using various models based on the impulse approximation. The results are consistent with the existence of a *universal* scaling function, which means that $f(\psi)$ is basically the same for different types of reactions, such as (e, e') and (ν, μ) , provided that the same kinematical regime is considered. As a consequence, instead of using specific models for the nuclear structure and reaction mechanism, one can use the *phenomenological* SuSA superscaling function extracted from (e, e') data to make reliable predictions for neutrino-nucleus cross sections. This strategy was first pursued in [14] for charge-changing (CC) (ν, μ) processes, and has recently been applied [15] to neutral-current (NC) neutrino-nucleus scattering reactions. In both cases, predictions were given for differential cross sections and a comparison with various relativistic FSI predictions was also provided for the two t -channel processes, (e, e') and (ν, μ) .

The differential cross sections and scaling functions were studied at depth in [6, 7, 14, 16], while in this work we focus on integrated cross sections. We present and discuss results for CC neutrino cross sections, integrated over the muon energy as a function of the muon scattering angle, as well as for cross sections integrated with respect to the scattering angle as a function of the outgoing muon energy. Finally, the behavior of the total cross section (integrated over both the scattering angle and muon energy) as a function of the incident neutrino energy is also investigated. We compare the results evaluated within the RIA framework with those obtained by using the *phenomenological* scaling function. We also include for reference the results corresponding to the relativistic Fermi gas (RFG) model.

Studies of integrated cross sections are relevant for the analysis of present and future neutrino oscillation experiments. The significant differences observed in the differential cross sections when comparing various model predictions [6, 7] with the phenomenological scaling function can also have consequences for the integrated cross sections. In particular, it is of interest to determine how the large *asymmetry* in the scaling function implied by the SuSA approach reflects on the integrated cross section. A comparison with the different theoretical descriptions, specifically the RMF approach which reproduces the asymmetry of data, may give us important clues on the validity of the diverse models.

In performing the analysis of integrated cross sections, an important issue refers to some of the kinematical regions accessed experimentally. In particular, small values of muon scattering angle between the incoming neutrino and the outgoing muon, θ_μ , imply small values of the momentum and energy transferred in the process. In this situation, a theoretical description of the reaction mechanism based on the impulse approximation is questionable. Fortunately, the contribution at these small angles to the global integrated cross section is negligible because

of the phase-space factor $\sin \theta_\mu$ entering the integral. Our aim here is to estimate the effects introduced in the integrated cross sections by different theoretical models and to compare these with those obtained by using the SuSA approach, and thus we integrate over the full range of θ_μ allowed by the kinematics.

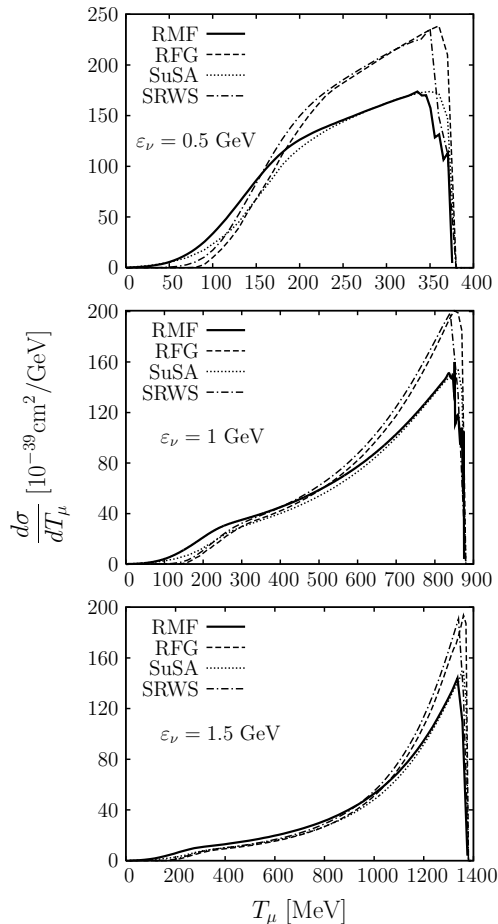


FIG. 1: CC cross section for ^{12}C integrated over the muon scattering angle as a function of the kinetic energy of the emitted muon. Results for RMF (solid), RFG (dashed), SuSA (dotted), and SRWS (dot-dashed) are compared for three different choices of kinematics.

In Fig. 1 we present results for the CC $^{12}\text{C}(\nu_\mu, \mu^-)$ cross section integrated over the muon scattering angle as a function of the muon kinetic energy. Predictions corresponding to the relativistic impulse approximation with FSI described with the RMF potential (solid line) are compared with the cross sections evaluated by making use of the phenomenological superscaling function $f(\psi)$ (dotted line), labelled SuSA. We also show results obtained in the RFG model (dashed line) and in the SR approach described in [16] using a Woods Saxon potential (dot-dashed line) denoted as SRWS. The parameters of the WS potential have been taken from [16], but with the depth of the central part of the proton potential adjusted

to reproduce the experimental mass difference between ^{12}C and ^{12}N . In the RMF and SRWS approaches the experimental energies for the bound neutrons are used, whereas in the SuSA and RFG approaches we have taken into account the mass difference between the initial and final nuclear systems, in accord with with Eq. (6) in [14]. This cuts out the higher muon kinetic energies and produces a depletion of the cross sections.

Three different values of the incident neutrino energy have been considered: $\varepsilon_\nu = 0.5, 1$ and 1.5 GeV. The relativistic plane-wave limit for the final nucleons, i.e., no FSI considered (not shown in the figure), leads to cross sections which are close to the RFG curves. Results in Fig. 1 show that the inclusion of FSI in SuSA and RMF gives rise to a significant shift of strength: the cross section increases the RFG result at lower muon energy values, whereas it quenches it at higher energies. This reduction, similar for both RMF and SuSA approaches, is about 20–25% in the region close to the maximum. In contrast, the SR model gives results that are similar to those of the RFG. Note also that the use of real potentials for describing the final nucleon states leads to the resonant structure observed for high T_μ (that is, small energy transfer ω).

In Fig. 2 we present the cross section integrated over the muon kinetic energy as a function of the muon scattering angle. Again we compare results for RMF (solid line), RFG (dashed), SuSA (dotted) and SRWS (dot-dashed). The inclusion of FSI in RMF and SuSA gives rise to a depletion of the cross section, except for very small angles.

As we show in the following, this implies a *smaller* global integrated cross section, which means that, besides the significant redistribution of strength produced by FSI, a global reduction is also observed when an integral over the muon energy and scattering angle is performed.

From Figs. 1 and 2 it appears that the SuSA and RMF approaches yield very similar results, corresponding to a redistribution of strength with respect to the RFG and SR models, in agreement with what was found in [6] and [16] for the double-differential cross sections. Note also that nuclear model effects are more important for lower neutrino energies ($\varepsilon_\nu = 0.5$ GeV), in accord with previous work [5, 17], and that the scaling arguments are only valid for high enough values of the transfer momentum q , i.e., for high enough values of the neutrino energy. Hence, some caution must be exercised when using the SuSA approach for small ε_ν .

Finally, nuclear model and FSI effects in the fully integrated cross section are presented in Fig. 3, where the total cross section σ is plotted as a function of the incident neutrino energy. Besides the four models considered in the previous figures we also display the result corresponding to RPWIA. All of the descriptions lead to a similar behavior for the quasielastic cross section, which increases with the neutrino energy up to $\varepsilon_\nu \sim 1$ – 1.2 GeV and then saturates to an almost constant value [5, 18].

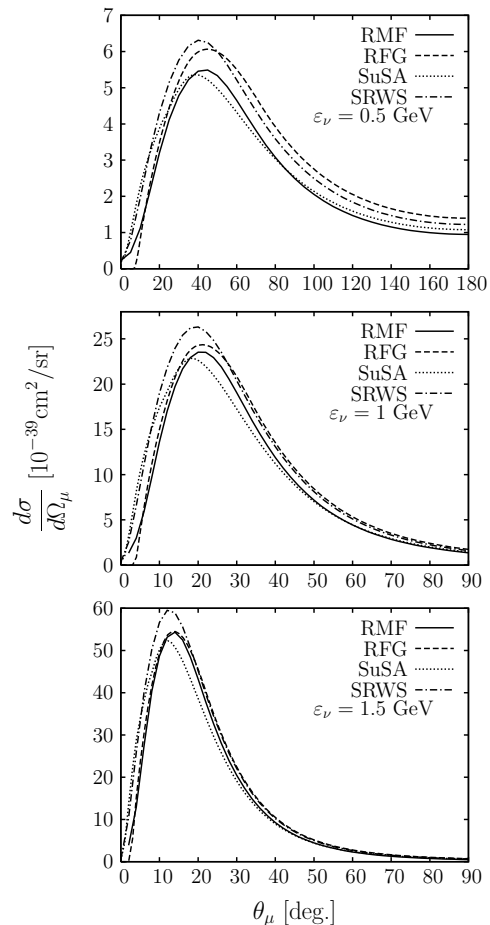


FIG. 2: Cross sections for the reaction $^{12}\text{C}(\nu_\mu, \mu^-)$ integrated over the emitted muon energy as a function of the scattering angle θ_μ for three values of the incident neutrino energy ε_ν . Results obtained within the context of the RIA and FSI described through the RMF (solid lines) and SRWS (dot-dashed) approaches are compared with the RFG model (dashed) and with the cross section obtained by using the phenomenological superscaling function extracted from the analysis of (e, e') world data, denoted by SuSA (dotted line).

We observe that the RPWIA and RFG models give very similar results up to $\varepsilon_\nu \simeq 0.8$ – 1 GeV, while for higher energies the RFG yields a lower cross section due to the above-mentioned nuclear mass difference, which entails a cut in the lower energy transfers. The SRWS model yields results which are close to the RFG prediction. The results denoted SRWS-tot include also the contribution of the discrete spectrum of ^{12}N obtained with the WS potential. This contribution turns out to be very small (below 2%). On the other hand, the RMF prediction coincides with the SuSA one up to neutrino energies of about 1.2 GeV. Moreover, the FSI effects in RMF and SuSA remain sizeable even at large ε_ν . In fact, they tend to stabilize, being of the order of $\sim 15\%$ at neutrino energies $\varepsilon_\nu \geq 1.2$ GeV.

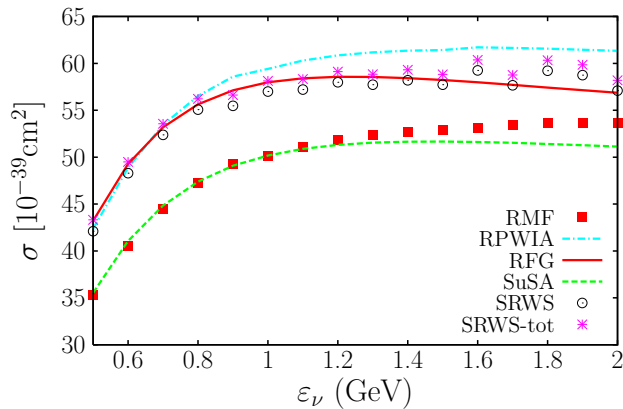


FIG. 3: (Color online) Total integrated CC cross section σ for QE muon neutrino reactions with ^{12}C as a function of the incident neutrino energy. We present results corresponding to RMF (squares), RFG (solid line), SuSA (dashed line), RPWIA (dot-dashed line), SRWS (circles) and SRWS-tot (crosses).

Before concluding, a comment is in order concerning the effect of Pauli blocking (PB) in the RFG model. It is well-known that PB, which is obviously accounted for in the RFG model, only affects the low momentum and energy transfer region. However in the process we are considering here this region is kinematically forbidden due to the mass difference between the initial (^{12}C) and residual (^{12}N) nuclei. As a consequence the effect of PB in the integrated cross sections turns out to be negligible.

In conclusion, we have evaluated the charged-current

quasielastic neutrino-nucleus cross sections integrated over the muon scattering variables (kinetic energy and scattering angle) within different relativistic theoretical approaches. Our results can be summarized as follows: (i) The effect of nuclear interactions is sizable for all values of the neutrino energy ranging from 0.5 to 2 GeV and amounts to a significant redistribution of the strength in the single-differential cross sections and to a lowering by about 15–20% of the total cross section with respect to the relativistic Fermi gas result. (ii) At high neutrino energies the differential cross section $d\sigma/d\theta_\mu$ is strongly peaked at low scattering angles; similarly $d\sigma/dT_\mu$ displays a pronounced maximum at high muon kinetic energy. As a consequence the total cross section is rather sensitive to the range of integration, which should be carefully taken into account when comparing with experimental data. (iii) Finally, the integrated cross section evaluated with the phenomenological superscaling function is very close to the RMF prediction. This result complements our previous analyses of differential cross sections and scaling functions, and it gives us confidence in the adequacy of descriptions of QE (ν_μ, μ) reactions within the RIA context when FSI are included via strong relativistic potentials.

Acknowledgements

This work was partially supported by Ministerio de Educación y Ciencia (Spain) and FEDER funds, under Contracts Nos. FPA2005-04460, FIS2005-01105, BFM2005-00810, by the Junta de Andalucía, and by the INFN-CICYT collaboration agreement N° 05-22. It was also supported in part (TWD) by U.S. Department of Energy under cooperative agreement No. DE-FC02-94ER40818.

-
- [1] J.M. Udías *et al.*, Phys. Rev. C **48**, 2731 (1993); **51**, 3246 (1995); **64**, 024614-1 (2001).
[2] Y. Jin, D.S. Onley and L.E. Wright, Phys. Rev. C **45**, 1333 (1992); K.S. Kim and L.E. Wright, Phys. Rev. C **68**, 027601 (2003); **72**, 064607 (2005).
[3] C.R. Chinn, A. Picklesimer and J.W. Van Orden, Phys. Rev. C **40**, 790 (1989).
[4] E.D. Cooper, S. Hama, B.C. Clark and R.L. Mercer, Phys. Rev. C **47**, 297 (1993).
[5] C. Maieron, M.C. Martínez, J.A. Caballero and J.M. Udías, Phys. Rev. C **68**, 048501 (2003).
[6] J.A. Caballero, J.E. Amaro, M.B. Barbaro, T.W. Donnelly, C. Maieron and J.M. Udías, Phys. Rev. Lett. **95**, 252502 (2005).
[7] J.A. Caballero, Phys. Rev. C **74**, 015502 (2006).
[8] Y. Horikawa, F. Lenz and N. C. Mukhopadhyay, Phys. Rev. C **22**, 1680 (1980).
[9] A. Meucci, F. Capuzzi, C. Giusti and F.D. Pacati, Phys. Rev. C **67**, 054601 (2003).
[10] T.W. Donnelly and I. Sick, Phys. Rev. Lett. **82**, 3212 (1999).
[11] T.W. Donnelly and I. Sick, Phys. Rev. C **60**, 065502 (1999).
[12] C. Maieron, T.W. Donnelly and I. Sick, Phys. Rev. C **65**, 025502 (2002).
[13] J.E. Amaro, M.B. Barbaro, J.A. Caballero, T.W. Donnelly and J.M. Udías, submitted to Phys. Rev. C.
[14] J.E. Amaro, M.B. Barbaro, J.A. Caballero, T.W. Donnelly, A. Molinari and I. Sick, Phys. Rev. C **71**, 015501 (2005).
[15] J.E. Amaro, M.B. Barbaro, J.A. Caballero, T.W. Donnelly, Phys. Rev. C **73**, 035503 (2006).
[16] J.E. Amaro, M.B. Barbaro, J.A. Caballero, T.W. Donnelly and C. Maieron, Phys. Rev. C **71**, 065501 (2005).
[17] W.M. Alberico *et al.*, Nucl. Phys. A **623**, 471 (1997).
[18] M.C. Martínez, P. Lava, N. Jachowicz, J. Ryckebusch, K. Vantournhout and J.M. Udías, Phys. Rev. C **73**, 024607 (2006).